



## Application of rotational resonance to inhomogeneously broadened systems

Jonathan Heller<sup>a</sup>, Russell Larsen<sup>b,c,1</sup>, Matthias Ernst<sup>b</sup>, Andrew C. Kolbert<sup>b,d,2</sup>,  
Michael Baldwin<sup>d</sup>, Stanley B. Prusiner<sup>d</sup>, David E. Wemmer<sup>b,e</sup>, Alexander Pines<sup>b,c</sup>

<sup>a</sup> Graduate Group in Biophysics, University of California, Berkeley, CA 94720, USA

<sup>b</sup> Department of Chemistry, University of California, Berkeley, CA 94720, USA

<sup>c</sup> Materials Sciences Division, Lawrence Berkeley Laboratory, Berkeley, CA 94720, USA

<sup>d</sup> Department of Neurology, University of California, San Francisco, CA 94143, USA

<sup>e</sup> Structural Biology Division, Lawrence Berkeley Laboratory, Berkeley, CA 94720, USA

Received 11 December 1995; in final form 23 January 1996

### Abstract

A protocol is presented for the determination of internuclear distances using rotational-resonance magnetization-exchange NMR in systems with inhomogeneously broadened lines. Non-linear least-square fitting procedures are used to obtain the distance, the inhomogeneous broadening, the zero-quantum relaxation time, and error estimates for these parameters. We apply this procedure to a biological system of unknown structure.

### 1. Introduction

Reintroduction of dipolar couplings into solid-state nuclear magnetic resonance (NMR) magic-angle spinning (MAS) spectra has become an important method for the measurement of distances in polycrystalline solids [1]. Homonuclear [2–4] and heteronuclear [5–7] dipolar couplings can be reintroduced through pulse sequences or, for homonuclear spin pairs, by matching the spinning speed to the difference of the isotropic chemical shifts, a particularly useful technique known as rotational-resonance

magnetization exchange [8,9]. To date, rotational resonance has produced reliable results in systems where the measured distances are known a priori, and error estimates have been derived by comparison with the known distances. The general utility of this technique is dependent on the ability to determine the zero-quantum relaxation times and to account for the effects of inhomogeneously broadened single-quantum transitions. Since the magnetization transfer caused by rotational resonance not only depends on the distance between spins but also on the rotational-resonance condition and the zero-quantum relaxation, it is important to take account of the impact of each parameter and to develop an approach for estimating errors.

In this paper, we describe a modified simulation program, including inhomogeneous broadening,

<sup>1</sup> Present address: Department of Chemistry, University of Iowa, Iowa City, IA 52242, USA.

<sup>2</sup> Present address: DSM Copolymer, P.O. Box 2591, Baton Rouge, LA 70821, USA.

which is used to fit the rotational-resonance exchange curves, giving well defined errors of the distance ( $r_{cc}$ ), the transverse zero-quantum relaxation time ( $T_{2ZQ}$ ), and the inhomogeneous linewidth ( $\Delta\nu_{1/2}$ ; full width at half height). For short distances,  $r_{cc} \leq 3.5$  Å, magnetization-exchange curves show resolved oscillations and the correlation between parameters is low, allowing simultaneous optimization of all three parameters. For long distances, however, no resolved oscillations are observed in the magnetization exchange, and the parameters are highly correlated. In these cases, we propose the use of the optimized values of  $T_{2ZQ}$  and  $\Delta\nu_{1/2}$ , obtained from a short distance measurement under similar conditions, to fit only  $r_{cc}$ .

## 2. Theory and simulations

The theory of rotational-resonance experiments has been extensively discussed previously [9]. The relevant part of the homonuclear coupled two-spin system can be described as a fictitious spin-1/2 using Bloch-type equations in a reduced three by three Liouville space [10]. In our work  $T_{2ZQ}$  relaxation was included in the simulations;  $T_1$  relaxation was assumed to be much longer and was therefore neglected. The simulation of the time-dependent Liouvillian was implemented using Floquet theory [11–13] using the NMR simulation environment GAMMA [14]. Powder averages were performed using the method of Cheng et al. [15] to obtain an optimal coverage of the sphere. Inhomogeneous broadening of the single-quantum transitions was introduced into the simulations by stepping the chemical-shift difference from the rotational-resonance condition with weightings appropriate to a Lorentzian lineshape. The chemical-shielding tensor values were fixed at values taken from the literature [16], while the orientation of the three principle axes with respect to the dipolar coupling was fixed at a random orientation. The  $J$ -coupling value was assumed to be 0 Hz. It has been shown that when the spinning speed equals the chemical-shift difference (i.e. the  $n = 1$  rotational-resonance condition), magnetization exchange is relatively insensitive to the chemical-shielding tensor values and its orientation [17,18].

The simulation program was integrated into a non-linear least-square optimization routine, which allowed us to simultaneously optimize  $r_{cc}$ ,  $T_{2ZQ}$  and  $\Delta\nu_{1/2}$ , or any subset of these parameters [18–20]. Statistical errors and cross-correlation coefficients, as well as error potentials and surfaces were calculated. For the optimizations, typical parameters were 18 time points, 200 different powder orientations, and a Floquet space truncated to a dimension of seven. Inhomogeneity was included by stepping the chemical-shift difference through ten values, up through three linewidths. The correlation between the chemical shift inhomogeneity of the two lines was determined by fitting this linewidth. If the chemical shifts of the two lines were completely correlated, the linewidth obtained would be zero, while if the two lines were completely uncorrelated, the resulting linewidth would equal the observed linewidth, i.e. the correlation of the chemical shift inhomogeneity of the two lines is reflected in the ratio of the observed linewidth and fit linewidth. A three-parameter optimization on an SGI Indigo [2] with a MIPS R4000 processor typically took several hours. For a one-parameter optimization of  $r_{cc}$ , optimization time was 30 min on the same computer.

## 3. Experimental

A home-built spectrometer operating at a  $^1\text{H}$  Larmor frequency of 301.2 MHz and a Chemagnetics (Fort Collins, CO) 4-mm double resonance high-speed spinning probe were used for all experiments. Spinning speeds were controlled to  $\pm 10$  Hz with long-term stability, using a home-built spinning-speed controller using a phase-locked loop. CP contact time was 2.5 ms, the  $^1\text{H}$  decoupling field strength was 100 kHz, and recycle delays were 5 s.

All experiments were carried out on three doubly labeled 14-residue peptides, with the sequence MKHMAGAAAAGAVV [21]. The first sample (sample I) was  $^{13}\text{C}$  labeled at the carbonyl of glycine-6 and  $\text{C}_\alpha$  of alanine-7, with a distance of  $r_{cc} = 2.4$  Å. The second sample (sample II) was labeled at the carbonyl of alanine-5 and  $\text{C}_\alpha$  of alanine-7, providing an  $r_{cc}$  between 4.5 and 5.4 Å, depending on the conformation of the peptide. Sample II was diluted to 10% in natural abundance

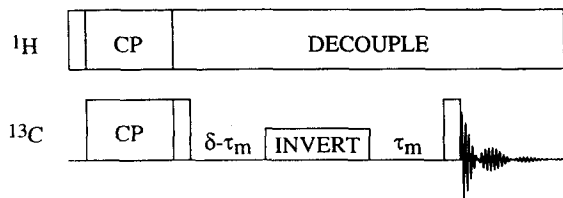


Fig. 1. Pulse sequence used for rotational-resonance experiments. After cross-polarization the magnetization is stored in the  $z$ -direction and the on-resonance component is inverted by a weak rf pulse or a DANTE sequence. A variable length delay ( $\delta - \tau_m$ ) is inserted before the inversion to keep the total experiment time constant, independent of  $\tau_m$ . After the delay  $\tau_m$  magnetization is returned to the  $x$ - $y$  plane for detection. During the experiment, the sample is spun at the magic angle with the frequency set to the difference of the isotropic chemical shifts of the two lines. High-power proton decoupling is applied after cross-polarization for the duration of the experiment.

background to reduce intermolecular effects, which are insignificant for sample I. Sample III, used for hole burning experiments, was  $^{13}\text{C}$  labeled at the carbonyl of alanine-7 and  $\text{C}_\alpha$  of glycine-6, with an  $r_{cc}$  between 4.4 and 4.7 Å.

The pulse sequence used for rotational-resonance magnetization exchange is shown in Fig. 1. After cross-polarization from protons to carbon, the carbon magnetization was stored along the  $z$ -axis and proton decoupling was turned on for the duration of the experiment. A variable delay ( $\delta - \tau_m$ ) was inserted before the selective inversion to keep the total experiment time constant [20]. This led to the same power dissipation due to proton decoupling in all experiments, independent of  $\tau_m$ , eliminating radio-frequency (rf) heating effects as a source of error in measurements. The on-resonance carbon magnetization was inverted with either a weak cw pulse or a DANTE sequence [22] and after a variable-length mixing time,  $\tau_m$ , a carbon read pulse returned the magnetization to the  $x$ - $y$  plane for detection. During the entire experiment, the sample was spun at the magic angle at a frequency that was equal to the isotropic chemical shift difference between the  $^{13}\text{C}$  labeled peaks.

Data were acquired as follows. At least 256 scans were acquired at the beginning of each experiment and discarded in order to allow the spectrometer and probe to stabilize. A cycle of data collection consisted of 32 or 64 scans acquired for each of the 18

mixing times  $\tau_m$ , with the time points in random order. These cycles were repeated many times. For each experiment, the spectral regions occupied by the  $^{13}\text{C}$  labels and a region occupied by natural-abundance resonances, resolved from the labeled peaks, were integrated separately. These integrals were used to calculate the experimental mean and standard deviation of the spectral amplitudes for the full data set.

The integral of the natural-abundance peak was monitored to ensure that all intensity changes are due to magnetization exchange rather than experimental artifact [23]. The natural-abundance peak was also used to estimate the natural-abundance contribution to each of the  $^{13}\text{C}$  labeled peaks, since in general the natural-abundance isochromats do not undergo magnetization exchange at the same rate as the isotopically labeled nuclear pair. The natural-abundance contribution was subtracted from the integral of the labeled peak before statistical analysis and calculation of the difference magnetization. This subtraction was carried out using the integrals of identical spectral regions in both labeled and natural-abundance samples with spectra normalized in spectral regions resolved from resonances due to isotopic labels.

In order to determine if inhomogeneity values determined by fits were realistic, hole-burning experiments (Fig. 2) were carried out on sample III, spinning at the magic angle at a frequency matching the  $n = 1$  rotational-resonance condition for the chemical-shift difference between peak maxima. A

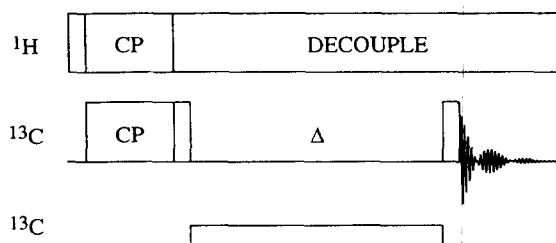


Fig. 2. Pulse sequence used for hole-burning experiments. After cross-polarization, the magnetization is stored along the  $z$ -direction and a weak rf field is irradiated at the carbonyl frequency for  $\Delta = 80$  ms. The magnetization is then returned to the  $x$ - $y$  plane for detection. During the experiment, the sample is spun at the magic angle with the frequency set to the difference of the isotropic chemical shifts of the two lines. High-power proton decoupling is applied after cross-polarization for the duration of the experiment.

separate frequency synthesizer was used to generate very low-power rf ( $\gamma B_1/(2\pi) \approx 30$  Hz) that could be coupled into the probe. Two experiments were performed. After cross-polarization, magnetization was stored along the  $z$ -axis, and, in the first experiment, the low-power rf was turned on for 80 ms, with its frequency set to the center of the carbonyl resonance frequency. In the control experiment, the low-power rf was not used. In both cases, a read pulse was then applied, and the signal detected. In the hole-burning experiment, the long, weak rf pulse saturated a line within the carbonyl resonance whose linewidth was determined by  $T_2$  of the line. Because the rotational-resonance condition was met, this saturation was transferred to the spins of the  $C_\alpha$  peak that were coupled to the spins being saturated. By subtracting the hole-burning experiment from the control, the shapes of the burned and transferred holes were obtained. If the lines were completely correlated, the linewidth of the transferred hole would be determined by  $T_2$  of the  $C_\alpha$  resonance, but if the lines were completely uncorrelated (randomly correlated), the linewidth of the transferred hole would be the product of the inhomogeneous linewidth and the linewidth of the rotational-resonance condition. If the lines were partially correlated, the linewidth would fall between these two values.

#### 4. Evaluation of data and discussion

Fits of the inhomogeneous linewidth always resulted in values greater than zero but less than the observed linewidth, indicating partial, but not complete, correlation of the chemical-shift inhomogeneity of the two lines. The importance of including the inhomogeneous linebroadening into the simulations is clearly demonstrated in Fig. 3a. The best fit for a short distance (sample I) without inclusion of the inhomogeneous broadening ( $\Delta\nu_{1/2} = 0$  Hz, dashed line) fits the measured data very poorly, while inclusion of the inhomogeneity (solid line) improves the fit from  $\chi^2 = 3052$  to  $\chi^2 = 49$ . The fitted parameters also differ considerably. For the two-parameter fit, we obtain  $r_{cc} = 2.229 \pm 0.009$  Å and  $T_{2ZQ} = 0.89 \pm 0.03$  ms, while for the three-parameter fit, we obtain  $r_{cc} = 2.370 \pm 0.046$  Å,  $T_{2ZQ} = 9.54 \pm 0.41$  ms, and  $\Delta\nu_{1/2} = 77 \pm 3$  Hz. For the short distance,

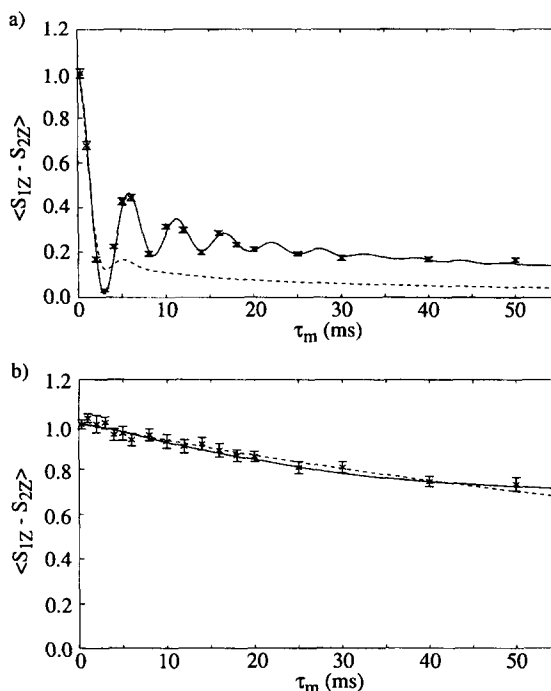


Fig. 3. Experimental and simulated rotational-resonance magnetization-exchange curves for (a) a short distance ( $r_{cc} \approx 2.4$  Å, sample I) and (b) a long distance ( $r_{cc} \approx 4.5$  Å, sample II). The measurement for the short distance (a) shows well resolved oscillations. The best two-parameter fit (dashed line) with  $\Delta\nu_{1/2} = 0$  Hz does not agree at all with the experimental data, while the three-parameter fit (solid line) agrees very well with the measured points. The measurement for the long distance (b) shows only a multiexponential decay but no oscillations. In this case both the two-parameter fit of  $r_{cc}$  and  $T_{2ZQ}$  (dashed line,  $\Delta\nu_{1/2} = 0$ ) and the one-parameter fit of  $r_{cc}$  (solid line,  $\Delta\nu_{1/2}$  and  $T_{2ZQ}$  set to optimized values from the short distance fit) give good agreement with the experimental data, but the two-parameter fit gives unrealistic values of the fit parameters.

the parameters were largely uncorrelated, [ $\rho(\Delta\nu_{1/2}, r_{cc}) = 0.4$ ,  $\rho(\Delta\nu_{1/2}, T_{2ZQ}) = 0.6$ , and  $\rho(T_{2ZQ}, r_{cc}) = 0.5$ ]. This can also be seen from the plot of the  $\chi^2$  error surfaces as a function of the three parameters (Fig. 4a). In the case of completely uncorrelated parameters, one would expect a circle in these plots [24]. The surfaces observed are only slightly elliptical. Therefore, the simultaneous optimization of all three parameters gives meaningful results.

For a long distance (sample II) the three-parameter fit yields no meaningful results due to the high correlation [ $\rho(\Delta\nu_{1/2}, r_{cc}) = 0.99$ ,  $\rho(\Delta\nu_{1/2}, T_{2ZQ}) = 0.82$ , and  $\rho(T_{2ZQ}, r_{cc}) = 0.88$ ] of the parameters,

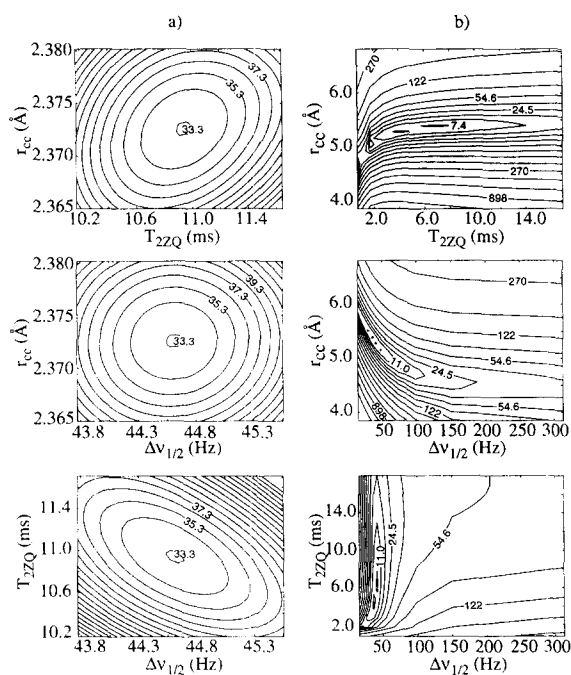


Fig. 4. Two-dimensional error surfaces showing  $\chi^2$  as a function of the three different fit parameters  $r_{cc}$ ,  $\Delta\nu_{1/2}$ , and  $T_{2ZQ}$  for (a) a short distance and (b) a long distance. For the short distance, all three correlation coefficients are small [ $\rho(\Delta\nu_{1/2}, r_{cc}) = 0.4$ ,  $\rho(\Delta\nu_{1/2}, T_{2ZQ}) = 0.6$ , and  $\rho(T_{2ZQ}, r_{cc}) = 0.5$ ], resulting in largely undistorted error ellipses. The long distance shows high correlations [ $\rho(\Delta\nu_{1/2}, r_{cc}) = 0.99$ ,  $\rho(\Delta\nu_{1/2}, T_{2ZQ}) = 0.82$ , and  $\rho(T_{2ZQ}, r_{cc}) = 0.88$ ] resulting in highly distorted error ellipses in the error surface plots.

so simultaneous optimization of all three parameters is not possible. The high correlation of the parameters is clearly demonstrated in the  $\chi^2$  error surfaces (Fig. 4b) as a function of the three variable parameters showing error surfaces that are strongly distorted ellipses. Although inhomogeneity is present in the system, a good two-parameter fit (assuming no inhomogeneity) of rotational-resonance data for a long distance is possible (Fig. 3b, dashed line), due to the high correlation of parameters [ $\rho(T_{2ZQ}, r_{cc}) = 1.00$ ]. However, such fits give unrealistic values and large error margins for fitted parameters:  $r_{cc} = 4.558 \pm 1.35$  Å,  $T_{2ZQ} = 0.53 \pm 0.97$  ms and  $\chi^2 = 8.3$ . In order to overcome this problem we propose to use the optimized values for  $\Delta\nu_{1/2}$  and  $T_{2ZQ}$  obtained from the fit of the short distance in a one-parameter fit of  $r_{cc}$ . The transferability of these parameters

should be a valid assumption if the samples are prepared under similar conditions, and have similar homogeneous and inhomogeneous linewidths. The one-parameter fit (using  $T_{2ZQ} = 9.54$  ms and  $\Delta\nu_{1/2} = 77$  Hz obtained from peptide I) results in a distance of  $r_{cc} = 5.399 \pm 0.064$  Å (Fig. 3b, solid line). The  $\chi^2$  of this one-parameter fit is 7.7 compared to a  $\chi^2$  of 6.7 for the three-parameter fit.

Presumably the best solution to the correlated parameter problem would be to measure  $T_{2ZQ}$  and  $\Delta\nu_{1/2}$  independently. The zero-quantum relaxation time is difficult to measure and, so far, approximations have been used to calculate  $T_{2ZQ}$  based on the  $T_2$  values of the two involved spins [25]. Recently, however, experiments designed to measure  $T_{2ZQ}$  directly have been reported [26]. The correlation between inhomogeneous lines  $\Delta\nu_{1/2}$  is also difficult to measure and will be discussed in more detail.

For short distances, errors are determined by the three-parameter fit, and we report errors as two standard deviations, giving an  $r_{cc}$  for sample I between 2.28 and 2.46 Å, bracketing the true value of 2.40 Å. Error bounds for the longer distance measurements are calculated by putting bounds on the zero-quantum relaxation time and the inhomogeneity. To obtain a lower bound for the distance consistent with an experimental data set, a one-parameter fit of the distance was run setting  $T_{2ZQ}$  equal to the shortest estimated value and using the largest reasonable degree of inhomogeneous broadening. The upper bound for the distance came from a one-parameter fit of the distance, using the longest reasonable  $T_{2ZQ}$  value and the smallest reasonable amount of inhomogeneous broadening. The maximum  $T_{2ZQ}$  was taken to be 1.5 times the fit  $T_{2ZQ}$ , while the minimum was estimated from the single-quantum  $T_2$  values [25]. The maximum inhomogeneity was taken to be the linewidth of the broader of the two peaks, while its minimum was taken to be 0 Hz. This leads to an  $r_{cc}$  for sample II between 4.94 and 7.18 Å.

The inhomogeneous linewidth derived from fits of short distances indicate that the C=O and C $_{\alpha}$  lines are partially correlated. Hole-burning experimental results (Fig. 5) confirm these results. The hole burned by the low-power rf has a linewidth of 63 Hz, which is nearly the measured homogenous linewidth of the carbonyl ( $44 \pm 6$  Hz) found from a CPMG experiment [27,28]. The linewidth of the transferred hole

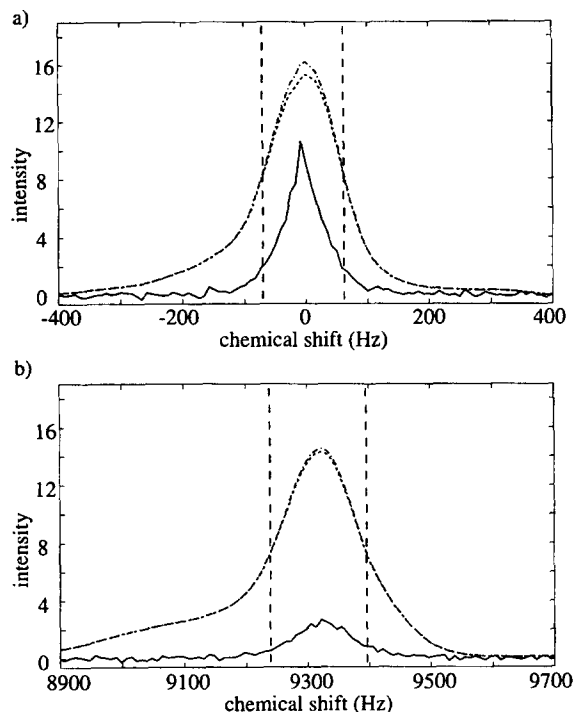


Fig. 5. Experimental results of holeburning experiments for sample III. The hole-burned spectrum (---), taken with the low-power  $^{13}\text{C}$  rf during the delay  $\Delta$ , is subtracted from the control spectrum (- · -), taken without the low-power rf. Vertical dashed lines indicate the half height of the control spectrum. Ten times the difference spectrum (—) shows the shape of the hole burned and of the hole transferred. (a) An expansion of the carbonyl region. The difference spectra shows the shape of the hole burned by the low-power rf. Its linewidth is 63 Hz, which is approximately the width of the homogeneous line ( $44 \pm 6$  Hz). (b) An expansion of the  $\text{C}_\alpha$  region. The difference spectrum shows the hole transferred by rotational resonance. Its width is 95 Hz, which is between the linewidth of the homogeneous line ( $48 \pm 6$  Hz) and the linewidth of the inhomogeneous line (151 Hz).

(95 Hz) is somewhat larger than the real homogeneous linewidth of the  $\text{C}_\alpha$  ( $48 \pm 6$  Hz), but is smaller than the full inhomogeneous linewidth (151 Hz). This result clearly demonstrates that some inhomogeneity exists in the chemical-shift difference, but also suggests that the shift difference is at least partially correlated. This experimental result is consistent with results obtained through parameter fitting, and supports our position that inhomogeneity should be included in the simulations and that our method of simulating inhomogeneity is acceptable.

## 5. Conclusions

We have described a protocol for using rotational-resonance magnetization exchange to determine distances in inhomogeneously broadened systems. Short-distance measurements were used to determine the zero-quantum relaxation time and the degree of correlation of chemical-shift inhomogeneity in the sample through three-parameter fits, and these parameters were then used as constants in one-parameter fits for the longer distances. Errors were calculated by putting bounds on our estimates of these two parameters and doing one-parameter fits of the distance to obtain maximum and minimum possible distances. We believe that the incorporation of fitting procedures with explicit protocols for obtaining numerical error bounds is useful for the study of internuclear distances and structures by rotational-resonance magnetization-exchange techniques.

## Acknowledgements

The work in Berkeley was funded by the Director, Office of Energy Research, Office of Basic Energy Sciences, Materials Sciences Division, U.S. Department of Energy, under Contract No. DE-AC03-76SF0098. The research at UCSF was supported by NIH (NS14069, AG08967, AG02132, NS22786), the American Health Assistance Foundation, the Sherman Fairchild Foundation, and the Bernard Osher Foundation. J.H. gratefully acknowledges the Howard Hughes Medical Institute for a predoctoral fellowship. M.E. thanks the Deutsche Forschungsgemeinschaft for the postdoctoral fellowship (Grant Er214/1-1). We also thank Professor Steve Smith, Yale University, and Professor Ann McDermott, Columbia University, for providing us with preprints, and Dr. Malcolm Levitt, Universitet Stockholm, for helpful discussions.

## References

- [1] A.E. Bennett, R.G. Griffin and S. Vega, *NMR: Basic Princ. Progr.* 33 (1994) 1.

- [2] C.S. Yannoni and R.D. Kendrick, *J. Chem. Phys.* 74 (1981) 747.
- [3] R. Tycko and G. Dabbagh, *Chem. Phys. Letters* 173 (1990) 461.
- [4] Y. Ishii and T. Terao, *J. Magn. Reson.* 115 (1995) 116.
- [5] B. Herzog and E.L. Hahn, *Phys. Rev.* 103 (1956) 148.
- [6] T. Gullion and J. Schaefer, *J. Magn. Reson.* 81 (1989) 196.
- [7] A.W. Hing, S. Vega and J. Schaefer, *J. Magn. Reson.* 96 (1992) 205.
- [8] D.P. Raleigh, M.H. Levitt and R.G. Griffin, *Chem. Phys. Letters* 146 (1988) 71.
- [9] M.H. Levitt, D.P. Raleigh, R. Creuzet and R.G. Griffin, *J. Chem. Phys.* 92 (1990) 6347.
- [10] R.R. Ernst, G. Bodenhausend and A. Wokaun, *Principles of nuclear magnetic resonance in one and two dimensions*, (Clarendon Press, Oxford, 1987).
- [11] J.H. Shirley, *Phys. Rev. B* 138 (1965) 979.
- [12] S. Vega, *J. Chem. Phys.* 96 (1992) 2655.
- [13] T.O. Levante, M. Baldus, B.H. Meier and R.R. Ernst, *Mol. Phys.* 86 (1995) 1195.
- [14] S.A. Smith, T.O. Levante, B.H. Meier and R.R. Ernst, *J. Magn. Reson.* A106 (1994) 75.
- [15] V.B. Cheng, H.H. Suzukawa and M. Wolfsberg, *J. Chem. Phys.* 59 (1973) 3992.
- [16] T.M. Duncan, *A compilation of chemical shift anisotropies*, (The Farragut Press, Chicago, 1990).
- [17] D.P. Raleigh, F. Creuzet, S.K. Das Gupta, M.H. Levitt and R.G. Griffin, *J. Am. Chem. Soc.* 111 (1989) 4502.
- [18] L.K. Thompson, A. McDermott, J. Raap, C.M. van der Wielen, J. Lugtenburg, J. Herzfeld and R.G. Griffin, *Biochemistry* 31 (1992) 7931.
- [19] F. Creuzet, D.P. Raleigh, M.H. Levitt and R.G. Griffin, *J. Am. Chem. Soc.* (in press).
- [20] Y. Tomita, E.J. O'Connor and A. McDermott, *J. Am. Chem. Soc.* 116 (1994) 8766.
- [21] S.B. Prusiner, *Biochemistry* 31 (1992) 12277.
- [22] G.A. Morris and R. Freeman, *J. Magn. Reson.* 29 (1978) 433.
- [23] O. Peerson, M. Groesbeek, S. Aimoto and S.O. Smith, *J. Am. Chem. Soc.* 117 (1995) 7228.
- [24] A.A. Clifford, *Multivariate error analysis*, (Applied Science Publishers, London, 1973).
- [25] A. Kubo and C.A. McDowell, *J. Chem. Soc. Faraday Trans.* 1 84 (1988) 3713.
- [26] Y. Tomita and A. McDermott, *ENC*, 1995, Boston, MA.
- [27] H.Y. Carr and E.M. Purcell, *Phys. Rev.* 94 (1954) 630.
- [28] S. Meiboom and D. Gill, *Rev. Sci. Instr.* 29 (1958) 688.